Rock and Soil Mechanics

Volume 41 | Issue 9 Article 4

2-8-2021

A creep constitutive model for transversely isotropic rocks

Lie-lie LI
School of Civil Engineering and Communication, North China University of Water Resources and Electric Power, Zhengzhou, Henan 450045, China

Jun-feng GUAN
School of Civil Engineering and Communication, North China University of Water Resources and Electric Power, Zhengzhou, Henan 450045, China, junfengguan@ncwu.edu.cn

Ming-li XIAO
State Key Laboratory of Hydraulics and Mountain River Engineering, Sichuan University, Chengdu, Sichuan 610065, China

Hai-chao LIU
School of Civil Engineering and Communication, North China University of Water Resources and Electric Power, Zhengzhou, Henan 450045, China

See next page for additional authors

Custom Citation

LI Lie-lie, GUAN Jun-feng, XIAO Ming-li, LIU Hai-chao, TANG Ke-dong, . A creep constitutive model for transversely isotropic rocks[J]. Rock and Soil Mechanics, 2020, 41(9): 2922-2930.

Rock and Soil Mechanics 2020 41(9): 2922−2930 ISSN 1000−7598
https: //doi.org/10.16285/j.rsm.2019.6387 rocksoilmech.researchcommons.org/journal

A creep constitutive model for transversely isotropic rocks

LI Lie-lie[1], GUAN Jun-feng[1], XIAO Ming-li[2], LIU Hai-chao[1], TANG Ke-dong[1]

1. School of Civil Engineering and Communication, North China University of Water Resources and Electric Power, Zhengzhou, Henan 450045, China
2. State Key Laboratory of Hydraulics and Mountain River Engineering, Sichuan University, Chengdu, Sichuan 610065, China

Abstract: Due to the presence of bedded or jointed planes, layered rock mass shows transversely isotropic characteristics in mechanics. Therefore, the existing isotropic creep model is difficult to fully reflect the creep constitutive model of transversely isotropic rock mass. In order to obtain the three-dimensional transversely isotropic creep constitutive model, the Burgers model is adopted to describe the characteristics of instantaneous strain, decaying creep and steady creep of transversely isotropic rock mass. Based on the assumption of constant Poisson's ratio and three-dimensional isotropic creep constitutive equation, a three-dimensional creep constitutive equation of transversely isotropic rock mass is derived through differential operator method by substitution of transversely isotropic compliance matrix into isotropic compliance matrix. The new model also takes the differences of creep behaviours between specimens with horizontally and vertically oriented bedding into account. According to the characteristics of creep constitutive equation, a method for identifying the creep parameters in the three-dimensional creep constitutive model is proposed based on the creep test results. The model is applied to the identification of triaxial creep test parameters, and a comprehensive set of three-dimensional creep parameters are obtained. The rationality of the proposed creep equation is verified by comparing theoretical values with experiment results. The limitations of the traditional creep tests design scheme are further pointed out and some suggestions for creep tests design of transversely isotropic materials are given. The research results provide a new insight for the study of three-dimensional creep mechanism of rock mass and provide scientific support for the design of rock mass creep tests.

Keywords: transversely isotropic; three dimensional model; creep equation; parameter identification

1 Introduction

The rock mass in nature is generally characterized by strong heterogeneity, especially in the environment of well developed joints and karst, underground water seepage and tectonic events, where the rock mass exhibits time-dependent anisotropic mechanical behavior. Even for isotropic rocks, they are mostly affected by engineering factors such as excavation, and thus their creep mechanical behavior is also anisotropic. Generally, the creep mechanical analysis of rock mass starts from the observation of creep phenomenon, followed by the exploration of creep mechanism from microscopic or macroscopic view, and then use abstract mathematical model to construct the corresponding creep constitutive model. Layered rocks extensively deposit in the earth's crust and have the characteristics of transverse isotropy in mechanics. With the development of underground engineering, the mechanical properties of layered rock, especially creep properties, cast an important influence on the deformation and stress distribution of surrounding rock in tunnels, underground hydropower and other projects. The key to describe the creep characteristics of layered rock mass is to construct a reasonable creep constitutive model[1−2], which can guide the practical engineering problems accurately and effecttively. Therefore, it is of great scientific significance and engineering application value to study the creep constitutive model of layered rock mass.

The research of creep constitutive model of rock mass has always been a hot topic of international and domestic scholars. The creep models of transversely isotropic materials published abroad can be divided into two categories, namely the empirical model which is summarized by experimental phenomena and the theoretical model which is obtained by plastic theory. Park et al.[3] took the weakening effect of elastic shear modulus over time into account and constructed the creep constitutive model of transversely isotropic rock. However, their empirical model regards the nonlinear behavior of elasticity as viscosity, which is not a viscosity model in real sense. Berman et al.[4] assumed that the failure behavior of materials was ideal plasticity, and derived the anisotropic creep constitutive equation that could reflect the stable creep stage under triaxial loading. Furthermore, Lliboutry[5], Aravas et al.[6], Robinson[7] deduced more complex transversely isotropic models and anisotropically rheological

Received: 12 August 2019 Revised: 22 March 2020
This work was supported by the National Natural Science Foundation of China(51779095), the Youth Fund of China Natural Science Foundation(5170090818) and the Science Technology Innovation Talents in Universities of Henan Province(20HASTIT013).
First author: LI Lie-lie, male, born in 1983, PhD, Lecturer, mainly engaged in the research on rock concrete materials and structures. E-mail: 13370912@qq.com
Corresponding author: GUAN Jun-feng, male, born in 1980, PhD, Professor, mainly engaged in the research on fracture mechanics of rock concrete. E-mail: junfengguan@ncwu.edu.cn

models based on the dissipative potential function. However, the creep constitutive model of anisotropy theory is mainly based on the plastic theory, which is more applicable to deal with the materials with plastic failure, such as metals. It is well known that failure of rock mass exhibits quasi-brittleness rather than complete plasticity. Therefore, the research on the anisotropically viscoelastic plastic element model that is suitable for describing the quasi-brittle fracture failure of rock mass can reflect the failure nature of rock mass more accurately. At present, it is urgent to carry out corresponding research on this issue.

It is generally considered that creep deformation of rock mass is a combination of elastic, viscous and plastic properties, each of which is represented by a specific component. The creep characteristics at different stages can be described by the combination of different components. Due to its clear physical meaning of each component, this method has been widely used. Currently, scholars in China mainly use shear creep test, uniaxial compression creep test, triaxial compression creep test, numerical simulation and theoretical analysis to carry out the corresponding research on layered rock mass. The weak bedding plane is an inherent factor of anisotropy for transversely isotropic rock. Therefore, Zhang et al.[8] and Li et al.[9] conducted shear creep tests on sandstone samples with weak bedding planes. A one-dimensional 4-component creep model and a one-dimensional Burgers model with water content were established, respectively. Based on the shear creep results of greenschist containing weak planes, Zhang et al.[10] connected a nonlinear shear creep component with the Nishihara model in series, and developed one-dimensional nonlinear creep component models. Through the shear creep tests on layered rocks, it was found that his models can effectively reflect the creep characteristics of weak planes, although most of the creep models are one-dimensional. In order to establish 3-D creep model of layered rock mass, numerical simulations, uniaxial and triaxial compression creep tests were conducted by many scholars on slate[11], quartz-mica schist[12], shale[13], composite rock[14] and layered red sandstone[15]. On this basis, the one-dimensional component creep model is extended to the three-dimensional one by referring to the derivation of constant bulk modulus of isotropic rocks. Liu et al.[11], Xiao et al.[12], Tang et al.[13] and Xu et al.[14] adopted the 3D creep equation of constant bulk modulus. When fitting the creep parameters according to the creep test results, only axial strain rather than cyclic strain was considered, and the correlations of creep parameters with different bedding dip angles were not presented. According to the creep curve of layered red sandstone, Shan et al.[15] used constant bulk modulus three-dimensional creep equation to fit the creep parameters, taking into account the axial strain and circumferential strain at the same time. However, in their paper, the axial and circumferential creeps of the same specimen were simply fitted as independent creep parameters, and the correlation of creep parameters of rock mass with different bedding dip angles was not considered. It is clear that based on constant bulk modulus, the existing 3D creep models of layered rock identify the creep parameters in different directions as different independent values, but not real 3D creep constitutive model for transversely isotropic rock mass, which failed to achieve the goal of using a set of creep parameters to describe the creep characteristics of rock mass with different bedding inclinations. The reason is that the idea of constant bulk modulus assumption is to decompose the stress state of any point in the object into a spherical stress tensor and a deviatoric stress tensor. The spherical stress only induces spherical strain and the deviatoric stress only induces the deviatoric strain. However, this assumption is not valid in layered rock mass. Spherical stress and deviatoric stress tensors can induce spherical strain and deviatoric strain simultaneously because of its anisotropy[16]. Combining the component creep model with the transversely isotropic mechanical characteristics of layered rock so as to obtain a 3D creep constitutive model is still an important scientific problem that needs to be solved urgently. However, there are few references in the existing literature.

In this paper, the well known Burgers model is adopted. Based on the assumption of constant Poisson's ratio and 3D isotropic creep constitutive equation, a 3D creep constitutive equation of transversely isotropic rock mass is derived by substitution of transversely isotropic compliance matrix into isotropic compliance matrix. Based on the proposed model and identification method, the creep parameters of phyllite are obtained and the creep mechanism of transversely isotropic rock mass is revealed. Finally, according to the characteristics of creep equation, the proposal of creep test design scheme for transversely isotropic materials is given.

2 Establishment of 3D creep constitutive model

2.1 3D creep constitutive model of isotropic rock

Given the characteristics of the whole-process creep

DOI: 10.16285/j.rsm.2019.6387

test curve of layered rock mass[1−2], the 3D creep constitutive model should have the following characteristics: elastic component should be included to reflect the characteristics of instantaneous elasticity; a parallel combination of elastic and viscous components should be contained within the model to describe the decaying creep; the model should also contain viscous component to reflect the stable creep (or subaccelerated creep) of rock mass.

Based on the above analysis, the Burgers model composed of Maxwell body and Kelvin body in series (as shown in Fig. 1) was selected to describe the real creep characteristics of layered rock mass.

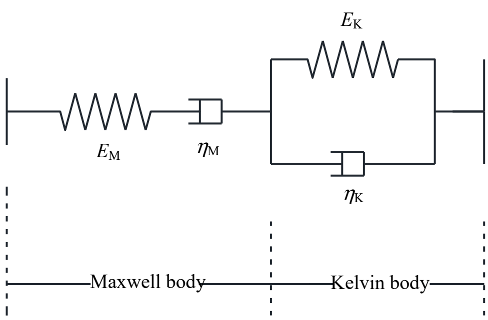

Fig. 1 Burgers model

The one-dimensional creep equation of Burgers model can be expressed as

$$\varepsilon=\left(\frac{1}{E_{\rm M}}+\frac{1}{\eta_{\rm M}D}+\frac{1}{E_{\rm K}+\eta_{\rm K}D}\right)\sigma \tag{1}$$

where $E_{\rm M}$ and $E_{\rm K}$ are elasticity modulus of Maxwell body and Kelvin body, respectively; $\eta_{\rm M}$ and $\eta_{\rm K}$ are coefficients of viscosity of Maxwell body and Kelvin body, respectively; σ is axial deviatoric stress; ε is axial creep deformation; and D is the integral operator.

The creep compliance tensor $J(t)$ can be written as

$$J(t)=\frac{1}{E_{\rm M}}+\frac{1}{\eta_{\rm M}D}+\frac{1}{E_{\rm K}+\eta_{\rm K}D} \tag{2}$$

Then Eq. (1) can be simplified into

$$\varepsilon=J(t)\sigma \tag{3}$$

Based on the creep constitutive equation derived under one-dimensional condition, the constitutive equation can be extended to 3D stress state by combining the relevant assumptions. Constant Poisson's ratio assumption is adopted in this study[17], indicating that the Poisson's ratio does not change with time and stress, and is equal to the Poisson’s ratio during elastic stage, $\mu(\sigma,t)=\mu$ [17]. For isotropic rocks, 3-D creep equation can be obtained by using creep compliance tensor substitution method as follows[18−19],

$$\{\varepsilon\}=J(t)[A]\{\sigma\} \tag{4}$$

where $[A]$ is the Poisson's ratio matrix of isotropic materials; $\{\varepsilon\}=\{\varepsilon_x,\varepsilon_y,\varepsilon_z,\gamma_{yz},\gamma_{xz},\gamma_{xy}\}^{\rm T}$; $\{\sigma\}=\{\sigma_x,\sigma_y,\sigma_z,\tau_{yz},\tau_{xz},\tau_{xy}\}^{\rm T}$. ε, γ, σ and τ are the normal strain, shear strain, normal stress and shear stress, respectively; Subscripts x, y, z and xz, yz, xy indicate the directions and planes in which the strain or stress are located. The specific meaning of each symbol can be found elsewhere[14−15].

2.2 Establishment of 3D creep constitutive model for transversely isotropic rock

Layered rock is characterized by transversely isotropic mechanical properties. A 3D cartesian coordinate system is presented in Fig.2. Assume that plane *xoy* is the transversely isotropic plane and axis *z* is perpendicular to plane *xoy*.

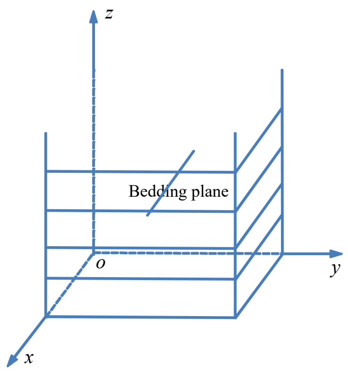

Fig. 2 Diagram of coordinate system

According to the coordinate system in Fig.2, the stress−strain constitutive relation of transversely isotropic rock in 3D stress state can be obtained as follows[20]:

$$\{\varepsilon\}=[S]\{\sigma\} \tag{5}$$

where

$$[S]=\begin{bmatrix}\frac{1}{E_{\rm h}} & -\frac{\mu_{\rm hh}}{E_{\rm h}} & -\frac{\mu_{\rm hv}}{E_{\rm v}} & 0 & 0 & 0\\ -\frac{\mu_{\rm hh}}{E_{\rm h}} & \frac{1}{E_{\rm h}} & -\frac{\mu_{\rm hv}}{E_{\rm v}} & 0 & 0 & 0\\ -\frac{\mu_{\rm hv}}{E_{\rm v}} & -\frac{\mu_{\rm hv}}{E_{\rm v}} & \frac{1}{E_{\rm v}} & 0 & 0 & 0\\ 0 & 0 & 0 & \frac{1}{G'} & 0 & 0\\ 0 & 0 & 0 & 0 & \frac{1}{G'} & 0\\ 0 & 0 & 0 & 0 & 0 & \frac{2(1+\mu_{\rm hh})}{E_{\rm h}}\end{bmatrix} \tag{6}$$

where E_{h} and E_{v} are the elastic modulus parallel and perpendicular to bedding direction, respectively; μ_{hh} and μ_{hv} are the Poisson's ratios parallel and perpendicular to bedding direction, respectively; G' is shear modulus perpendicular to bedding direction.

Transversely isotropic rock has five independent elastic parameters. Gonzaga et al.[21] reduced the independent elastic parameters to four and gave an approximate expression of the elastic parameters as

$$\frac{1}{G'}=\frac{1}{E_{\mathrm{h}}}+\frac{(1+2\mu_{\mathrm{hv}})}{E_{\mathrm{v}}} \tag{7}$$

Assume $E_{\mathrm{v}}=nE_{\mathrm{h}}$, where n is the ratio of E_{v} to E_{h}. Combined with Eq. (7), the compliance matrix in Eq. (5) can be written as

$$[S]=\frac{1}{E_{\mathrm{h}}}[U_{\mathrm{tra}}] \tag{8}$$

$$[U_{\mathrm{tra}}]=\begin{bmatrix} 1 & -\mu_{\mathrm{hh}} & -\frac{\mu_{\mathrm{hv}}}{n} & 0 & 0 & 0 \\ -\mu_{\mathrm{hh}} & 1 & -\frac{\mu_{\mathrm{hv}}}{n} & 0 & 0 & 0 \\ -\frac{\mu_{\mathrm{hv}}}{n} & -\frac{\mu_{\mathrm{hv}}}{n} & \frac{1}{n} & 0 & 0 & 0 \\ 0 & 0 & 0 & 1+\frac{1+2\mu_{\mathrm{hv}}}{n} & 0 & 0 \\ 0 & 0 & 0 & 0 & 1+\frac{1+2\mu_{\mathrm{hv}}}{n} & 0 \\ 0 & 0 & 0 & 0 & 0 & 2(1+\mu_{\mathrm{hh}}) \end{bmatrix} \tag{9}$$

For transversely isotropic rock, it is assumed that Poisson's ratio remains a constant with the change of stress and time, and is equal to the constant of the elastic stage. In this paper, the differential operator substitution method[18−19] is adopted to keep the Poisson's ratio matrix unchanged. Then the Poisson's ratio matrix [A] of isotropic materials in Eq. (4) is substituted by the Poisson's ratio matrix [U_{tra}] of transversely isotropic materials as shown in Eq. (8). Consequently, the 3-D creep constitutive equation for layered rock can be obtained as follows:

$$\{\varepsilon\}=J(t)[U_{\mathrm{tra}}]\{\sigma\} \tag{10}$$

Creep compliance in Eq. (10) is calculated by integration. Given the fact that the creep properties vary significantly parallel or perpendicular to bedding directions, n_1, n_2, n_2 and n_4 are introduced to replace the n in Poisson's ratio matrix of transversely isotropic materials, [U_{tra}]. The purpose of this manipulation is to reflect the difference between instantaneous creep elastic component, steady creep viscous component, elastic component and viscous component in delaying creep. Expanding Eq. (10), the following equation is yielded.

$$\begin{aligned}\varepsilon_x={}&\frac{1}{E_{\mathrm{M}}^{\mathrm{h}}}\left(\sigma_x-\mu_{\mathrm{hh}}\sigma_y-\frac{\mu_{\mathrm{hv}}}{n_1}\sigma_z\right)+\\&\frac{1}{\eta_{\mathrm{M}}^{\mathrm{h}}}\left(\sigma_x-\mu_{\mathrm{hh}}\sigma_y-\frac{\mu_{\mathrm{hv}}}{n_2}\sigma_z\right)t+\frac{1}{E_{\mathrm{K}}^{\mathrm{h}}}\left(\sigma_x-\mu_{\mathrm{hh}}\sigma_y-\frac{\mu_{\mathrm{hv}}}{n_3}\sigma_z\right)\cdot\\&\left\{1-\exp\left[-\frac{E_{\mathrm{K}}^{\mathrm{h}}\left(\sigma_x-\mu_{\mathrm{hh}}\sigma_y-\frac{\mu_{\mathrm{hv}}}{n_4}\sigma_z\right)}{\eta_{\mathrm{K}}^{\mathrm{h}}\left(\sigma_x-\mu_{\mathrm{hh}}\sigma_y-\frac{\mu_{\mathrm{hv}}}{n_3}\sigma_z\right)}t\right]\right\}\end{aligned} \tag{11}$$

$$\begin{aligned}\varepsilon_y={}&\frac{1}{E_{\mathrm{M}}^{\mathrm{h}}}\left(-\mu_{\mathrm{hh}}\sigma_x+\sigma_y-\frac{\mu_{\mathrm{hv}}}{n_1}\sigma_z\right)+\\&\frac{1}{\eta_{\mathrm{M}}^{\mathrm{h}}}\left(-\mu_{\mathrm{hh}}\sigma_x+\sigma_y-\frac{\mu_{\mathrm{hv}}}{n_2}\sigma_z\right)t+\frac{1}{E_{\mathrm{K}}^{\mathrm{h}}}\left(-\mu_{\mathrm{hh}}\sigma_x+\sigma_y-\frac{\mu_{\mathrm{hv}}}{n_3}\sigma_z\right)\cdot\\&\left\{1-\exp\left[-\frac{E_{\mathrm{K}}^{\mathrm{h}}\left(-\mu_{\mathrm{hh}}\sigma_x+\sigma_y-\frac{\mu_{\mathrm{hv}}}{n_4}\sigma_z\right)}{\eta_{\mathrm{K}}^{\mathrm{h}}\left(-\mu_{\mathrm{hh}}\sigma_x+\sigma_y-\frac{\mu_{\mathrm{hv}}}{n_5}\sigma_z\right)}t\right]\right\}\end{aligned} \tag{12}$$

$$\begin{aligned}\varepsilon_z={}&\left\{\frac{1}{E_{\mathrm{M}}^{\mathrm{h}}n_1}+\frac{1}{\eta_{\mathrm{M}}^{\mathrm{h}}n_2}t+\frac{1}{E_{\mathrm{K}}^{\mathrm{h}}n_3}\left[1-\exp\left(-\frac{E_{\mathrm{K}}^{\mathrm{h}}n_3}{\eta_{\mathrm{K}}^{\mathrm{h}}n_4}t\right)\right]\right\}\cdot\\&\left(-\mu_{\mathrm{hv}}\sigma_x-\mu_{\mathrm{hv}}\sigma_y+\sigma_z\right)\end{aligned} \tag{13}$$

$$\begin{aligned}\gamma_{yz}={}&\left\{\frac{1}{E_{\mathrm{M}}^{\mathrm{h}}}\left(1+\frac{1+2\mu_{\mathrm{hv}}}{n_1}\right)+\frac{1}{\eta_{\mathrm{M}}^{\mathrm{h}}}\left(1+\frac{1+2\mu_{\mathrm{hv}}}{n_2}\right)t+\right.\\&\left.\frac{1}{E_{\mathrm{K}}^{\mathrm{h}}}\left(1+\frac{1+2\mu_{\mathrm{hv}}}{n_3}\right)\left\{1-\exp\left[-\frac{E_{\mathrm{K}}^{\mathrm{h}}\left(1+\frac{1+2\mu_{\mathrm{hv}}}{n_4}\right)}{\eta_{\mathrm{K}}^{\mathrm{h}}\left(1+\frac{1+2\mu_{\mathrm{hv}}}{n_3}\right)}t\right]\right\}\right\}\tau_{yz}\end{aligned} \tag{14}$$

$$\begin{aligned}\gamma_{xz}={}&\left\{\frac{1}{E_{\mathrm{M}}^{\mathrm{h}}}\left(1+\frac{1+2\mu_{\mathrm{hv}}}{n_1}\right)+\frac{1}{\eta_{\mathrm{M}}^{\mathrm{h}}}\left(1+\frac{1+2\mu_{\mathrm{hv}}}{n_2}\right)t+\right.\\&\left.\frac{1}{E_{\mathrm{K}}^{\mathrm{h}}}\left(1+\frac{1+2\mu_{\mathrm{hv}}}{n_3}\right)\left\{1-\exp\left[-\frac{E_{\mathrm{K}}^{\mathrm{h}}\left(1+\frac{1+2\mu_{\mathrm{hv}}}{n_4}\right)}{\eta_{\mathrm{K}}^{\mathrm{h}}\left(1+\frac{1+2\mu_{\mathrm{hv}}}{n_3}\right)}t\right]\right\}\right\}\tau_{xz}\end{aligned} \tag{15}$$

$$\begin{aligned}\gamma_{xy}={}&\left\{\frac{1}{E_{\mathrm{M}}^{\mathrm{h}}}(2+2\mu_{\mathrm{hh}})+\frac{1}{\eta_{\mathrm{M}}^{\mathrm{h}}}(2+2\mu_{\mathrm{hh}})t+\right.\\&\left.\frac{1}{E_{\mathrm{K}}^{\mathrm{h}}}(2+2\mu_{\mathrm{hh}})\left\{1-\exp\left[-\frac{E_{\mathrm{K}}^{\mathrm{h}}(2+2\mu_{\mathrm{hh}})}{\eta_{\mathrm{K}}^{\mathrm{h}}(2+2\mu_{\mathrm{hh}})}t\right]\right\}\right\}\tau_{xy}\end{aligned} \tag{16}$$

where $E_{\mathrm{M}}^{\mathrm{h}}, \eta_{\mathrm{M}}^{\mathrm{h}}, E_{\mathrm{K}}^{\mathrm{h}}, \eta_{\mathrm{K}}^{\mathrm{h}}$ and the corresponding n_1, n_2, n_3,

n_4 are eight independent tensile and compression creep parameters perpendicular to bedding direction. It can be seen that, unlike 3D creep constitutive model of isotropic rock, the proposed 3D creep constitutive model of transversely isotropic rock takes the distinctions of creep mechanical behavior parallel and perpendicular to bedding directions into account. If the creep behaviors in those two directions are the same, namely $n_1 = n_2 = n_3 = n_4 = 1$, then Eqs. (11)−(16) are reduced to 3D creep constitutive model of isotropic rock.

3 Identification of creep parameters of transversely isotropic rock

In order to verify the rationality and applicability of the proposed model, triaxial compression creep tests of transversely isotropic rock were conducted. The phyllite used in the laboratory test was taken from the entrance of Taoping tunnel in Wenchuan County. The phyllite is a typical transversely isotropic rock mass with distinct layered structure. According to the different inclinations of the bedding planes, the original rock samples were processed into two types with horizontal bedding and vertical bedding, respectively. As shown in Fig. 3, the samples were all cylinders with a diameter of 5 cm and a height of 10 cm. Through uniaxial compression tests, μ_{hv} and μ_{hh} were calculated as 0.15 and 0.10 according to the method of Cho et al.[20].

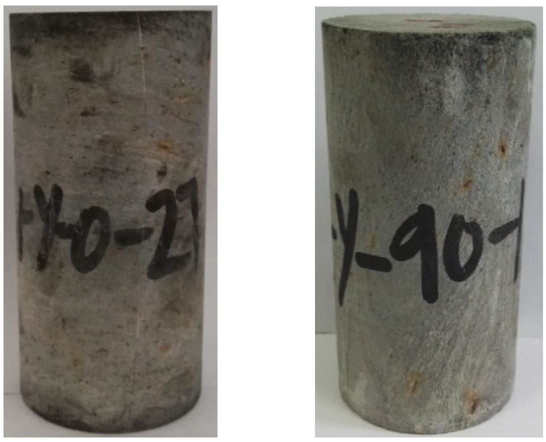

(a) Sample with horizontal bedding (b) Sample with vertical bedding

Fig. 3 Typical rock specimens

MTS815 rock mechanics testing system was used to perform conventional triaxial compression tests with a confining pressure of 5 MPa for horizontal and vertical bedding samples. The loading direction is illustrated in Fig. 4. Triaxial creep tests were carried out according to the 80% of the peak strength of the triaxial compression test. Creep tests under confining pressure of 5 MPa were performed in 5−6 stages. Constant confining stress and graded increased axial stress were used in the creep tests. For horizontal bedding sample, the axial stress was increased step by step as 9.4, 15.1, 20.8, 26.0 and 32.2 MPa. For vertical bedding sample, the graded increased axial stress were 26.0, 35.6, 45.6, 55.5, 65.4 and 75.1 MPa, respectively.

The results of the triaxial compression creep tests of the horizontal and vertical bedding samples were treated by Chen's Loading Method and Boltzmann linear superposition principle to further obtain the graded creep curves of the horizontal and vertical bedding samples, as shown in Fig. 5.

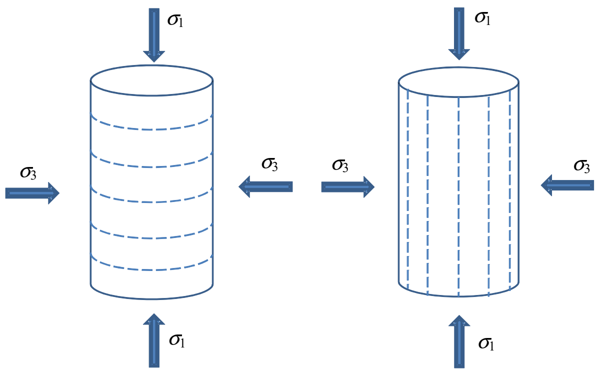

(a) Sample with horizontal bedding (b) Sample with vertical bedding

Fig. 4 Test rock specimens and loading directions

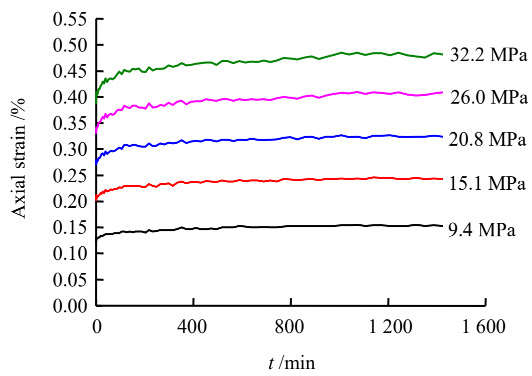

(a) Sample with horizontal bedding

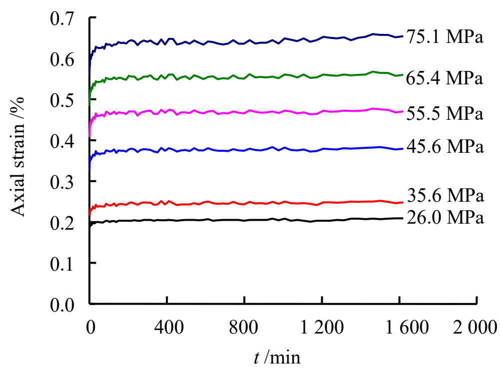

(b) Sample with vertical bedding

Fig. 5 Axial creep curves under different loading

Using the proposed 3D creep constitutive model for transversely isotropic rock, the principal stresses in *ox*, *oy* and *oz* directions in Fig.2 are noted as σ_x, σ_y and σ_z, respectively.

It can be found that for the case of vertical bedding, plane *xoy* is an isotropic plane, $\sigma_z=\sigma_y=\sigma_3$, $\sigma_x=\sigma_1$. $\varepsilon_{\text{Axial}}^{90}$ represents the axial strain of sample with vertical bedding, and then Eq. (11) can be rewritten as

$$\varepsilon_{\text{Axia}}^{90}=\frac{1}{E_{\text{M}}^{\text{h}}}(\sigma_1-\mu_{\text{hh}}\sigma_3)-\frac{\mu_{\text{hv}}}{E_{\text{M}}^{\text{h}}n_1}\sigma_3+\frac{1}{\eta_{\text{M}}^{\text{h}}}\cdot$$

$$(\sigma_1-\mu_{\text{hh}}\sigma_3)t-\frac{\mu_{\text{hv}}}{\eta_{\text{M}}^{\text{h}}n_2}\sigma_3 t+\left[\frac{1}{E_{\text{K}}^{\text{h}}}(\sigma_1-\mu_{\text{hh}}\sigma_3)-\frac{\mu_{\text{hv}}}{E_{\text{K}}^{\text{h}}n_3}\sigma_3\right]\cdot$$

$$\left\{1-\exp\left\{-\left\{\left[\frac{1}{\eta_{\text{K}}^{\text{h}}}(\sigma_1-\mu_{\text{hh}}\sigma_3)-\frac{\mu_{\text{hv}}\sigma_3}{\eta_{\text{K}}^{\text{h}}n_4}\right]\cdot\right.\right.\right.$$

$$\left.\left.\left.\left(\frac{1}{\dfrac{\sigma_1-\mu_{\text{hh}}\sigma_3}{E_{\text{K}}^{\text{h}}}-\dfrac{\mu_{\text{hv}}\sigma_3}{E_{\text{K}}^{\text{h}}n_3}}\right)\right\}t\right\}\right\} \tag{17}$$

Similarly, when the bedding plane is horizontal, plane *xoy* is an isotropic plane, $\sigma_x=\sigma_y=\sigma_3$, $\sigma_z=\sigma_1$. $\varepsilon_{\text{Axia}}^{0}$ represents the axial strain of horizontal bedding sample, and thus Eq. (13) can be written as

$$\varepsilon_{\text{Axia}}^{0}=\left\{\frac{1}{E_{\text{M}}^{\text{h}}n_1}+\frac{1}{\eta_{\text{M}}^{\text{h}}n_2}t+\frac{1}{E_{\text{K}}^{\text{h}}n_3}\left[1-\exp\left(-\frac{E_{\text{K}}^{\text{h}}n_3}{\eta_{\text{K}}^{\text{h}}n_4}t\right)\right]\right\}\cdot$$

$$\left(\sigma_1-2\mu_{\text{hv}}\sigma_3\right) \tag{18}$$

The flow chart of the identification of creep parameters developed in this study is displayed in Fig. 6. Note that σ_{H} is the stress level of horizontal bedding rock sample, and σ_{V} is the stress level of vertical bedding rock sample. Based on the analytical formula (Eq.(18)) and the creep test curves of horizontal bedding rock sample, the optimized parameter combinations, $E_{\text{M}}^{\text{h}}n_1, \eta_{\text{M}}^{\text{h}}n_2, E_{\text{K}}^{\text{h}}n_3$ and $\eta_{\text{K}}^{\text{h}}n_4$ can be obtained through Levenberg-Marquardt nonlinear least square fitting. Substitute these parameters into Eq. (17), and combined with the creep test curves results of vertical bedding rock, $E_{\text{M}}^{\text{h}}, \eta_{\text{M}}^{\text{h}}, E_{\text{K}}^{\text{h}}$ and $\eta_{\text{K}}^{\text{h}}$ are yielded through curve fitting. Consequently, n_1, n_2, n_3, and n_4 are calculated through the ratio of $E_{\text{M}}^{\text{h}}n_1$, $\eta_{\text{M}}^{\text{h}}n_2$, $E_{\text{K}}^{\text{h}}n_3$ and $\eta_{\text{K}}^{\text{h}}n_4$ to $E_{\text{M}}^{\text{h}}, \eta_{\text{M}}^{\text{h}}, E_{\text{K}}^{\text{h}}$ and $\eta_{\text{K}}^{\text{h}}$. It can be seen that the creep parameters identification method developed in this study is capable of displaying the creep characteristics of transversely isotropic rock mass in different bedding directions simultaneously via a unified set of creep parameters.

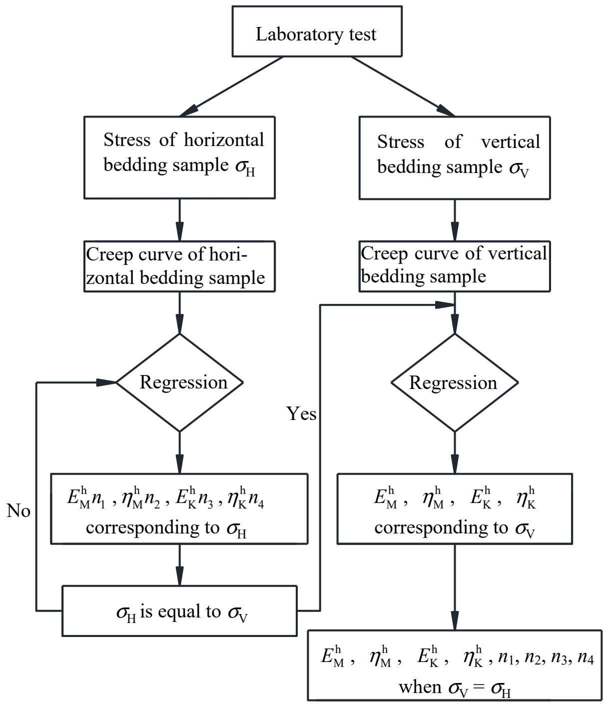

Fig. 6 Flow chart of creep parameter identification

According to the identification method of creep parameters and the creep test results of horizontal bedding rock sample, Eq.(18) is used for fitting analysis. The parameter combinations of horizontal bedding sample can be determined. Table 1 lists $E_{\text{M}}^{\text{h}}n_1$, $\eta_{\text{M}}^{\text{h}}n_2$, $E_{\text{K}}^{\text{h}}n_3$ and $\eta_{\text{K}}^{\text{h}}n_4$ under different stress levels (9.4, 15.1, 20.8, 26.0 and 32.2 MPa).

Table 1 Creep parameters of rock sample with horizontal bedding

Axial stress /MPa	$E_{\text{M}}^{\text{h}}n_1$ /GPa	$\eta_{\text{M}}^{\text{h}}n_2$ /(GPa • min)	$E_{\text{K}}^{\text{h}}n_3$ /GPa	$\eta_{\text{K}}^{\text{h}}n_4$ /(GPa • min)
9.4	7.1	244 155.8	42.5	1 066.2
15.1	7.2	230 887.1	50.0	2 020.5
20.8	7.5	214 212.5	53.0	2 259.5
26.0	7.8	163 580.2	52.1	1 858.9
32.2	8.1	157 073.5	50.8	1 390.2

The creep parameters of rock mass are related to its stress level. In this test, the triaxial stress of vertical bedding rock are 26.0, 35.6, 45.6, 55.5, 65.4 and 75.1 MPa, which are different from the stress of horizontal bedding rock(9.4, 15.1, 20.8, 26.0 and 32.2 MPa). Therefore, it is necessary to obtain the corresponding $E_{\text{M}}^{\text{h}}n_1, \eta_{\text{M}}^{\text{h}}n_2, E_{\text{K}}^{\text{h}}n_3$ and $\eta_{\text{K}}^{\text{h}}n_4$ of vertical bedding rock under the same stress levels through approximate calculation and regression analysis according to the results of horizontal bedding rock sample. In regression analysis, in order to avoid the presence of abnormal or even negative values as well as results distortion, linear and polynomial equations are generally not used in regression curve. The regression of creep parameters of horizontal bedding sample is shown in Fig. 7.

According to regression equation, $E_{\mathrm{M}}^{\mathrm{h}}n_1$, $\eta_{\mathrm{M}}^{\mathrm{h}}n_2$, $E_{\mathrm{K}}^{\mathrm{h}}n_3$ and $\eta_{\mathrm{K}}^{\mathrm{h}}n_4$ for vertical bedding sample under corresponding stress level are calculated. The results are listed in Table 2.

Substitute the results in Table 2 into Eq. (17), the creep parameters are available by fitting the creep curves of vertical bedding sample using Eq. (17), as shown in Table 3.

n_1, n_2, n_3 and n_4 can thus be calculated according to the prediction results in Table 2 and Table 3. Finally, eight independent creep parameters of transversely isotropic rock can be obtained, as shown in Table 4.

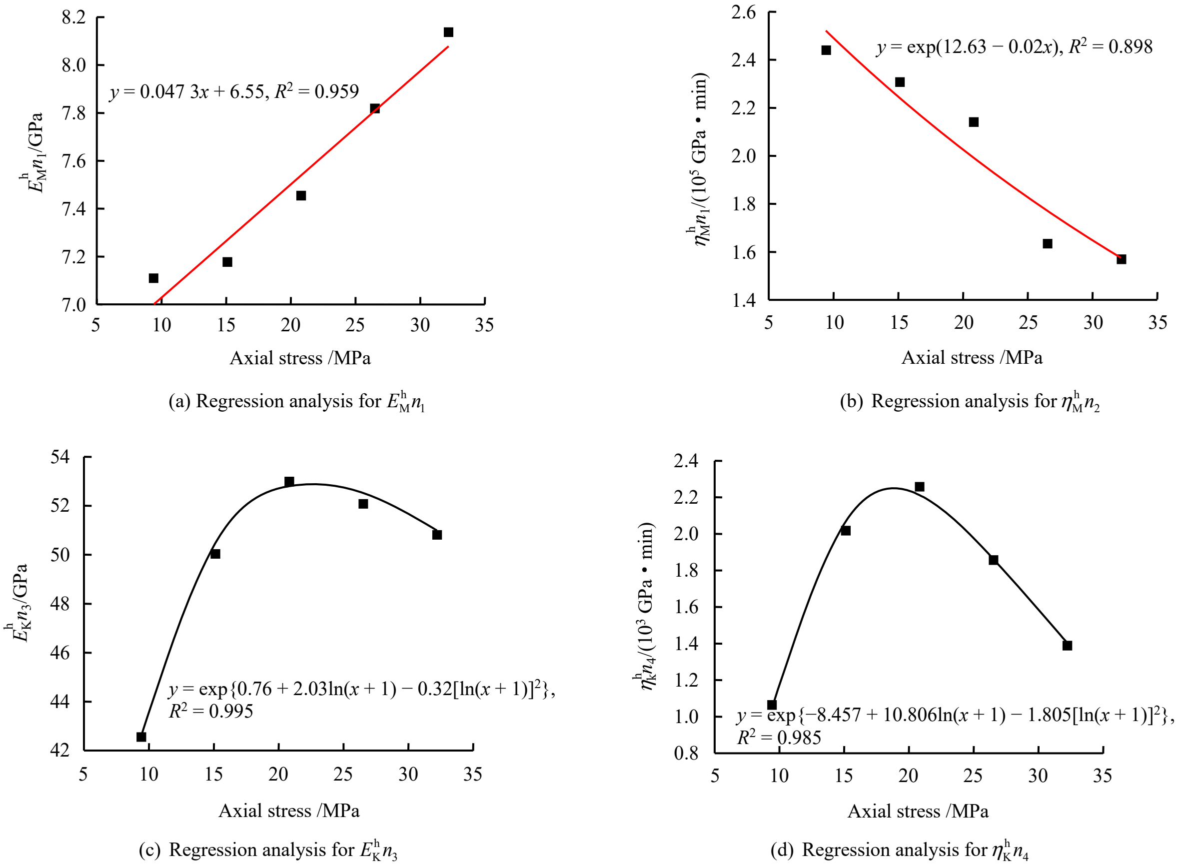

(a) Regression analysis for $E_{\mathrm{M}}^{\mathrm{h}}n_1$

(b) Regression analysis for $\eta_{\mathrm{M}}^{\mathrm{h}}n_2$

(c) Regression analysis for $E_{\mathrm{K}}^{\mathrm{h}}n_3$

(d) Regression analysis for $\eta_{\mathrm{K}}^{\mathrm{h}}n_4$

Fig. 7 Regression analysis of creep parameters

Table 2 List of calculated parameters

Axial stress /MPa	$E_{\mathrm{M}}^{\mathrm{h}}n_1$ /GPa	$\eta_{\mathrm{M}}^{\mathrm{h}}n_2$ /(GPa • min)	$E_{K}^{h}n_3$ /GPa	$\eta_{k}^{h}n_4$ /(GPa • min)
26.0	7.8	163 580.2	52.1	1 858.9
35.6	8.2	149 941.4	49.8	1 154.8
45.6	8.7	122 761.7	45.7	612.4
55.5	9.2	100 710.0	41.5	317.5
65.4	9.6	82 619.4	37.6	165.1
75.1	10.1	68 050.1	34.1	88.4

Table 3 List of parameters by curve fitting

Axial stress /MPa	$E_{\mathrm{M}}^{\mathrm{h}}n_1$ /GPa	$\eta_{\mathrm{M}}^{\mathrm{h}}n_2$ /(GPa • min)	$E_{K}^{h}n_3$ /GPa	$\eta_{K}^{h}n_4$ /(GPa • min)
26.0	13.4	1 421 417.6	165.6	3 373.0
35.6	15.8	957 550.7	158.3	3 337.0
45.6	13.1	970 913.0	141.6	2 247.0
55.5	13.0	662 534.4	127.6	1 704.0
65.4	12.9	645 590.9	133.7	207.4
75.1	12.9	365 808.3	131.1	188.7

Table 4 Creep parameters of layer vertical sample

Axial stress /MPa	$E_{\mathrm{M}}^{\mathrm{h}}$ /GPa	$\eta_{\mathrm{M}}^{\mathrm{h}}$ /(GPa • min)	$E_{\mathrm{K}}^{\mathrm{h}}$ /GPa	$\eta_{\mathrm{K}}^{\mathrm{h}}$ /(GPa • min)	n_1	n_2	n_3	n_4
26.0	13.44	1 421 418	165.6	3 373	0.58	0.12	0.31	0.55
35.6	15.75	957 551	158.3	3 337	0.52	0.16	0.31	0.35
45.6	13.13	970 913	141.6	2 247	0.66	0.13	0.32	0.27
55.5	12.95	662 534	127.6	1 704	0.71	0.15	0.33	0.19
65.4	12.92	645 591	133.7	207.4	0.74	0.13	0.28	0.80
75.1	12.91	365 808	131.1	188.7	0.78	0.19	0.26	0.47

Figure 8 compares the creep test values of phyllite with fitting values based on the model presented in this paper. It can be seen from Fig. 8, the values estimated by the 3-D creep constitutive equation are in good agreement with test values, indicating that the developed model is suitable for capturing the creep characteristics of phyllite.

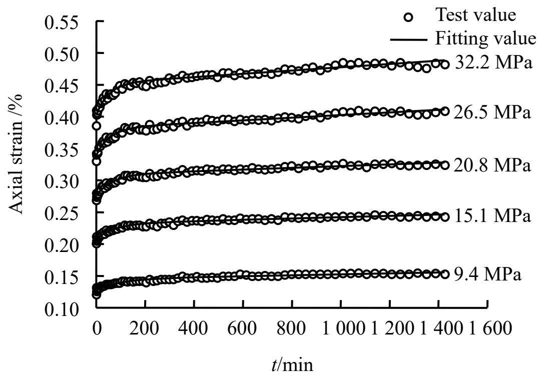

(a) Sample with horizontal bedding

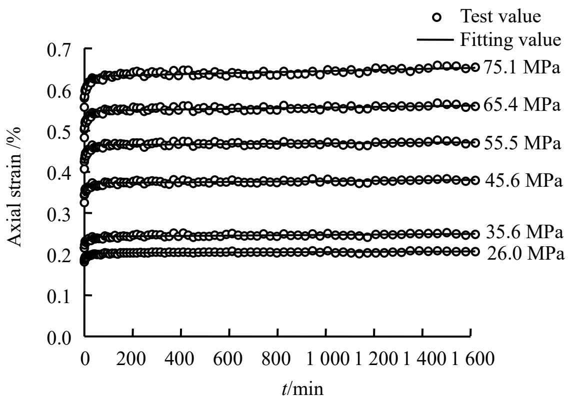

(b) Sample with vertical bedding

Fig. 8 Test creep curves of phyllite and curves fitting by developed model

4 Conclusions

Due to the existence of weak structure planes, the mechanical properties of layered rock mass and isotropic rock mass are significantly different. The creep characteristics of layered rock mass exhibit strong anisotropy. Therefore, it is difficult to describe the creep mechanical properties of transversely isotropic rocks using existing isotropic creep models. Based on the assumption of constant Poisson's ratio, a 3D creep constitutive model which can reflect the characteristics of transversely isotropic rock mass is derived, and an identification method of creep parameters for transversely isotropic rock mass is also developed according to the creep equation. The main conclusions can be drawn as follow:

(1) The creep curve of typical layered phyllite can be described by classic Burgers model, which presents the characteristics of instantaneous strain, decaying creep and steady creep. Based on the Burgers model and 3-D isotropic creep constitutive equation, with the aid of constant Poisson’s ratio, isotropic compliance matrix is replaced by transversely isotropic compliance matrix through differential operator method. Therefore, the creep constitutive equations of transversely isotropic materials with eight independent creep parameters are derived for the first time, which is capable of describing the characteristics of instantaneous strain, decaying creep and steady creep of transversely isotropic rock.

(2) According to the characteristics of the 3D creep equation of transversely isotropic rock, an identification method and implementation procedure of creep parameters are developed by equation transformation. Through creep tests on horizontal and vertical bedding samples under the same stress levels, eight creep parameters are calculated and analyzed. This method is powerful to display the creep characteristics of transversely isotropic rock in different bedding directions using a unified set of creep parameters.

(3) Based on the triaxial compression creep tests of phyllite with regards to horizontal and vertical bedding, eight creep parameters of the typical layered phyllite are obtained by using parameter identification method of 3-D creep equation. The rationality and applicability of the constitutive equation are verified by comparing model estimates with experimental results.

It should be noted that the conventional creep test design was adopted in the phyllite creep test. According to the load peak of phyllite with different bedding directions, the samples were loaded gradually with 5 to 6 stages with different stress levels by referring the 80% of peak strength. Creep properties and parameters of rock mass have close relationship with its stress level. Therefore, according to the developed creep constitutive model of transversely isotropic materials, it is suggested that creep test of horizontal and vertical bedding rock samples should be carried out at the same stress levels, as shown in Fig. 6, $\sigma_H = \sigma_V$, so that the creep parameters of transversely isotropic materials can be more accurately identified.

References

[1] ZHU Sai-nan, YIN Yue-ping, LI Bin. Shear creep behavior

of soft interlayer in Permian carbonaceous shale[J]. Rock and Soil Mechanics, 2019, 40(4): 1377−1386.

[2] CHEN Wen-wu, YUAN Peng-bo, LIU Xiao-wei. Study on creep properties of red-bed soft rock under step load[J]. Chinese Journal of Rock Mechanics and Engineering, 2009, 28(1): 3076−3081.

[3] PARK K, JUNG Y, CHUNG C. Evolution of stiffness anisotropy during creep of engineered silty sand in South Korea[J]. KSCE Journal of Civil Engineering, 2016, DOI: 10.1007/s 12205-016-1105-1.

[4] BERMAN I, PAI D H. A theory of anisotropic steady-state creep[J]. International Journal of Mechanical Sciences, 1966, 8(5): 341−352.

[5] LLIBOUTRY L. Anisotropic transversely isotropic nonlinear viscosity of rock ice and rheological parameters inferred from homogenization[J]. International Journal of Plasticity, 1993, 9(5): 619−632.

[6] ARAVAS N, CHENG C, CASTAŇEDA P P. Steady-state creep of fiber-reinforced composites: constitutive equations and computational issues[J]. International Journal of Solids and Structures, 1995, 32(15): 2219−2244.

[7] ROBINSON D N. Constitutive relationships for anisotropic high-temperature alloys[J]. Nuclear Engineering and Design, 1984, 83(3): 389−396.

[8] ZHANG Zhi-liang, XU Wei-ya, WANG Ru-bin, et al. Study of nonlinear viscoelasto-plastic rheological model of sandstone with weak plane[J]. Chinese Journal of Rock Mechanics and Engineering, 2011, 30(Suppl.1): 2634−2639.

[9] LI Peng, LIU Jian, ZHU Jie-bing, et al. Research on effects of water content on shear creep behavior of weak structural plane of sandstone[J]. Rock and Soil Mechanics, 2008, 29(7): 1865−1871.

[10] ZHANG Qing-zhao, SHEN Ming-rong, DING Wen-qi. Study of mechanical properties and long-term strength of jinping green schist[J]. Chinese Journal of Rock Mechanics and Engineering, 2012, 31(8): 1642−1649.

[11] LIU Xiao-jun, LIU Xin-rong, WANG Tie-hang, et al. Creep model of low-grade metamorphic slate considering moisture degradation effect[J]. Chinese Journal of Rock Mechanics and Engineering, 2014, 33(12): 2384−2389.

[12] XIAO Ming-li, ZHUO Li, XIE Hong-qiang, et al. Anisotropic rheological properties of quartz-mica schist under triaxial compression creep test[J]. Rock and Soil Mechanics, 2015, 36(2): 73−80.

[13] TANG Jian-xin, TENG Jun-yang, ZHANG Chuang, et al. Experimental study of creep characteristics of layered water bearing shale[J]. Rock and Soil Mechanics, 2018, 39(1): 33−41.

[14] XU Peng, YANG Sheng-qi. Numerical analysis of creep mechanical property for bedded composite rock[J]. Journal of Mining and Safety Engineering, 2018, 35(1): 179−187.

[15] SHAN Ren-liang, BAI Yao, SUN Peng-fei, et al. Study of triaxial creep mechanical properties and constitutive model of frozen stratified red sandstone[J]. Journal of China University of Mining and Technology, 2019, 48(1): 12−22.

[16] XIAO Ming-li. Study on rheological mechanical properties of transversely isotropic rock and its engineering[D]. Chengdu: Sichuan University, 2015.

[17] ZHU B. The stresses and deformations in the nonhomogeneous visco-elastic media undermixed boundary conditions[J]. Acta Mechanics Sinica, 1964, 7(2): 162−167.

[18] ZIENKIEWICZ O C, WATSON M, KING I P. A numerical method of visco-elastic stress analysis[J]. International Journal of Mechanical Sciences, 1968, 10: 807−827.

[19] HUANG Xiao-hua, FENG Xia-ting, CHEN Bing-rui, et al. Discussion on parameters determination of viscoelastic model in creep test[J]. Chinese Journal of Rock Mechanics and Engineering, 2007, 26(6): 1226−1231.

[20] CHO J W, KIM H, JEON S, et al. Deformation and strength anisotropy of Asan gneiss, Boryeong shale, and Yeoncheon schist[J]. International Journal of Rock Mechanics and Mining Sciences, 2012, 50(12): 158−169.

[21] GONZAGA G G, LEITE M H, CORTHÉSY R. Determination of anisotropic deformability parameters from a single standard rock specimen[J]. International Journal of Rock Mechanics and Mining Sciences, 2008, 45(8): 1420−1438.